Pigmentation is associated with stemness hierarchy of progenitor cells within cultured limbal epithelial cells

Liu, Lei; Nielsen, Frederik Mølgaard; Emmersen, Jeppe; Bath, Chris; Hjortdal, Jesper Østergaard; Riis, Simone; Fink, Trine; Pennisi, Cristian Pablo; Zachar, Vladimir

Published in:
Stem Cells

DOI (link to publication from Publisher):
10.1002/stem.2857

Publication date:
2018

Document Version
Publisher's PDF, also known as Version of record

Can I transform my understanding of **genomics, transcriptomics, and epigenomics** at single cell resolution?

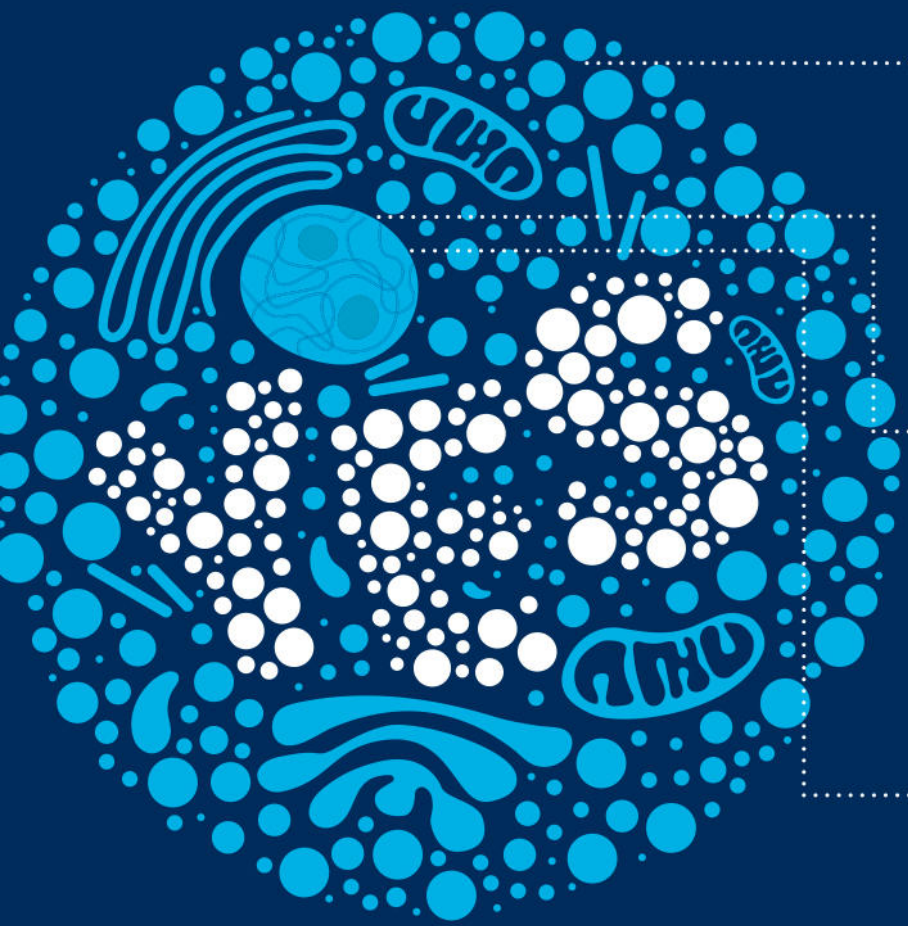

Uncover the full spectrum of cellular diversity and cellular interactions

Unmask true genetic diversity and map clonal evolution in complex disease

Unravel the epigenetic basis of disease and development cell by cell

Get a Multidimensional View of Complex Cellular Systems with Single Cell Solutions from 10x Genomics

Single Cell Transcriptomics

- Gene Expression Profiling
- Gene Expression CRISPR Screening
- Gene Expression & Cell Surface Protein
- Immune Profiling
- Immune Profiling & Cell Surface Protein
- Immune Profiling & Antigen Specificity

Single Cell Genomics

- Copy Number Variation

Single Cell Epigenomics

- Chromatin Accessibility

LEARN MORE AT 10XGENOMICS.COM/YES

10X GENOMICS

STEM CELLS®

TISSUE-SPECIFIC STEM CELLS

Pigmentation Is Associated with Stemness Hierarchy of Progenitor Cells Within Cultured Limbal Epithelial Cells

LEI LIU,[a,b] FREDERIK MØLGAARD NIELSEN,[a] JEPPE EMMERSEN,[a] CHRIS BATH,[c] JESPER ØSTERGAARD HJORTDAL,[d] SIMONE RIIS,[a] TRINE FINK,[a] CRISTIAN PABLO PENNISI,[a] VLADIMIR ZACHAR [a]

Key Words. Limbus corneae • Adult stem cells • Cells • Cultured • High-throughput nucleotide sequencing • Flow cytometry • Pigmentation

[a]Laboratory for Stem Cell Research, Department of Health Science and Technology, Aalborg University, Aalborg, Denmark; [b]Department of Pediatric Surgery, First Hospital of Jilin University, Changchun, Jilin, People's Republic of China; [c]Department of Ophthalmology, Aalborg University Hospital, Aalborg, Denmark; [d]Department of Ophthalmology, Aarhus University Hospital, Aarhus, Denmark

Correspondence: Vladimir Zachar, M.D., Ph.D., Fredrik Bajers Vej 3B, 9220 Aalborg East, Denmark. Telephone: (45) 99407556; e-mail: vlaz@hst.aau.dk

Received January 26, 2018; accepted for publication May 7, 2018; first published online in STEM CELLS *EXPRESS* May 20, 2018.

http://dx.doi.org/10.1002/stem.2857

ABSTRACT

Ex vivo cultured human limbal epithelial stem/progenitor cells (hLESCs) are the main source for regenerative therapy of limbal stem cell deficiency (LSCD), which is worldwide one of the major causes of corneal blindness. Despite many stemness-associated markers have been identified within the limbal niche, the phenotype of the earliest hLESCs has not been hitherto identified. We sought to confirm or refute the use of tumor protein p63 (p63) and ATP binding cassette subfamily B member 5 (ABCB5) as surrogate markers for hLESCs early within the limbal differentiation hierarchy. Based on a robust fluorescence-activated cell sorting and subsequent RNA isolation protocol, a comprehensive transcriptomic profile was obtained from four subpopulations of cultured hLESCs. The subpopulations were defined by co-expression of two putative stem/progenitor markers, the p63 and ABCB5, and the corneal differentiation marker cytokeratin 3. A comparative transcriptomic analysis yielded novel data that indicated association between pigmentation and differentiation, with the p63 positive populations being the most pigmented and immature of the progenitors. In contrast, ABCB5, either alone or in co-expression patterns, identified more committed progenitor cells with less pigmentation. In conclusion, p63 is superior to ABCB5 as a marker for stemness. STEM CELLS *2018;36:1411–1420*

SIGNIFICANCE STATEMENT

This study has first conducted a biomarker-oriented comparative transcriptomic analysis of cultured and sorted human limbal epithelial stem/progenitor cells (hLESCs), and found out that the p63 but not the ATP binding cassette subfamily B member 5 predicts the immaturity of niche progenitors. The comparative analysis of the functional gene networks furthermore revealed an association of stemness with pigmentation, which highlights the role of pigmentation in the protection of corneal limbus from radiation damage. These findings have implications for the acceptance and use of p63 as a marker for early hLESCs, and contribute to better understanding of hLESCs differentiation biology.

INTRODUCTION

The human limbal epithelial stem/progenitor cells (hLESCs) are believed to play a central role in renewing and repairing cornea [1]. However, this biological process may be disturbed thus leading to a condition termed limbal stem cell deficiency (LSCD). As a result, the cornea becomes opacified and vascularized, with a concomitant visual impairment that often results in complete blindness [2]. At present, transplantation of ex vivo cultured limbal epithelial cells is considered to be the most efficient treatment [2]. Since the first cultured limbal epithelial transplantation (CLET) was conducted in 1997 [3], thousands of CLET procedures have been reported from around the world [4]. Despite its indisputable success, the overall long-term success rate of this procedure does not surpass 80% [5–7]. Considerable effort is therefore currently being invested into better understanding of the biomolecular and developmental cues that control the limbal stem cell niche, so that the current CLET may be improved.

The hLESCs are usually identified by a combination of markers, which include p63, ABCG2, integrin α9, keratin 15, N-cadherin, NGF/TrkA, integrin α6/CD71, Hes1, p75, nectin 3, importin 13, nucleostemin, CD38/157, Lrig1,

ABCB5, and WNT7A [8]. Of special significance appears the p63 marker, since Pellegrini et al. in 2001 suggested that its deltaNp63α isoform is required to support the normal development of corneal epithelium [9]. Furthermore, the proportion of p63 positive cells in the limbal epithelial cell culture is a key factor influencing the success of CLET [5]. Consequently, it is being used as a surrogate marker for hLESCs in the world's first commercial stem cell product for the treatment of LSCD, the Holoclar [10, 11]. While this marker has a notable prognostic value, enrichment strategies based on antibody-sorting of cells are hindered by the fact that p63 is an intracellular protein. Alternatively, the ATP binding cassette subfamily B member 5 (ABCB5) surface protein, has been suggested as a putative hLESCs marker. Recent findings have shown that ABCB5 is critical for corneal epithelial homeostasis and repair [12] and it is often co-expressed with p63 in hLESCs both in situ [12] and ex situ [13, 14]. However, many concerns were recently raised regarding the ability of p63, as well as of ABCB5 to accurately detect hLESCs [11, 15, 16]. Thus, in spite of clear significance, the specific placement of these markers within the limbal differentiation hierarchy remains unresolved.

Earlier attempts to clarify the developmental biology and differentiation hierarchy of hLESCs have been hampered by the use of nondiscovery based methods such as microarray analysis [17–23], poor study material such as nonhuman or whole unfractionated tissue [24–29], or impure hLESC cultures [30, 31]. A few discovery based next-generation sequencing hLESCs transcriptomic studies have been conducted but these were also limited by the use of in situ material [32, 33] or nonhuman models [34–36].

To overcome these limitations, we have in this study combined our earlier optimized pipeline for high quality transcripts from human limbal epithelial cellular subpopulations sorted by fluorescence-activated cell sorting (FACS) [37] with discovery based next-generation sequencing. By using this strategy, we have as the first conducted a biomarker-oriented comparative transcriptome analysis of cultured and sorted hLESCs, and by this sought to refute or confirm the use of p63 and ABCB5 as surrogate markers for hLESCs.

Materials and Methods

Cell Culture

For isolation of hLESCs, corneal scleral rings were procured from the Danish Cornea Bank (Aarhus University Hospital, Arhus, Denmark) in accordance with the applicable Danish legislation. For a single isolation procedure, 10 to 12 randomly collected rings (donor age 22–86 years, 64% men, and absence of corneal disease) were used, and, altogether, three independent primary cell lines were established. The protocol for isolation and culture of hLESCs was based on our previous report [38]. In brief, after gross debridement and removal of the endothelium, the rings were incubated with 2.4 U/ml dispase II (Life Technologies, Naerum, Denmark) in sterile phosphate-buffered saline (sPBS; Gibco, Taastrup, Denmark) for 1 hour at 37°C. The limbal epithelial cell layer was then scraped and further digested with TrypLE (Gibco) for 15 minutes at 37°C. The obtained cell suspension was filtered through a 70 μm mesh (BD Biosciences, San Jose, CA), seeded into T25 culture flasks (Corning CellBIND, Sigma–Aldrich, Copenhagen, Denmark), and cultured in complete keratinocyte-SFM (Life Technologies). At 80%–90% confluency, the cells were detached using TrypLE for subsequent procedures.

In Situ Direct Immunofluorescence Assay

Live cell cultures at P2 to P3 were used to reveal the surface ABCB5 epitope (LifeSpan BioSciences, Seattle, WA), whereas cells fixed and permeabilized with 4% formaldehyde and 0.1% Triton X-100 (both from Sigma–Aldrich), respectively, were used to target the intracellular markers p63 and CK3 (both from US Biological, Salem, MA). Specifications of the used conjugates and their preimmune controls are listed in Supporting Information Table S1. The antibodies were diluted as recommended by manufacturers in sterile phosphate buffered saline (sPBS) supplemented with 10% fetal bovine serum (FBS) and 0.1% sodium azide in the case of unfixed cells, and incubated with the cells for 1 hour at 4°C. After a brief washing with PBS, the nuclei were stained with 0.1 μg/ml Hoechst 33342 for 10 minutes at 4°C., which was followed by the final washing and mounting in fluorescent mounting medium (DAKO, Glostrup, Denmark). The signal was visualized and recorded with Axio Observer.Z1 microscope (Carl Zeiss, Göttingen, Germany) equipped with Orca Flash 4.0 camera (Hamamatsu, Ballerup, Denmark). The images were processed using Zen (blue edition) software from Carl Zeiss. In additional experiments, the ABCB5 antibody was validated against previously established ABCB5 monoclonal (clone 5H3C6) [14] (data not shown).

Immunofluorescent Labeling for Cell Sorting

The experimental set up was previously optimized to reveal markers pertinent to this study using a set of directly labeled antibodies and to determine the sorting thresholds using matching isotype controls for p63 and CK3 and fluorescence minus one (FMO) for ABCB5 [39]. All buffers used in staining and subsequent FACS sorting were sPBS based, supplied with 50% Accumax (Sigma-Aldrich) and 25 mM HEPES (Life Technologies) to prevent cell clumping and to maintain a proper pH range. The cell suspensions were first stained for surface antigen ABCB5 at a working dilution of 1:50 for 30 minutes at 4°C, followed by washing, and then fixation and permeabilization with 70% ethanol (VWR, Herlev, Denmark) for 10 minutes at 4°C. After permeabilization, an Rnase inhibitor (Rnasin plus; Promega, Roskilde, Denmark) was utilized with each step. The intracellular antigens p63 and CK3 were targeted after additional washing with p63 (1:200) and CK3 (1:100), or with isotype controls for 30 minutes at 4°C. Finally, the labeled cells were transferred into a 5 ml round-bottom polystyrene tube (BD Falcon, Albertslund, Denmark) for the flow cytometric sorting and analysis. Using the previously established primary cell lines, three independent staining and sorting experiments were carried out.

FACS Cell Sorting

MoFlo Astrios cell sorter and Summit Software v4.3 (both from Beckman Coulter, Brea, CA) were used for both FACS and flow cytometric analysis. Gate strategies were set with reference to isotype and FMO controls, and discrimination limit for positive events was set at a fluorescence intensity higher than the top 2.5 percentile from the control samples. Before sorting, the

instrument was sequentially decontaminated with RNaze ZAP (Sigma-Aldrich), 70% ethanol, and milli-Q water. To minimize mechanical stress during sorting, system pressure was set at 20 psi, and a 100 μm sorting nozzle was used. FACS sorting was performed at 4°C, and it typically took 2 to 3 hours to complete. Four hLESCs phenotypic subpopulations, including p63+, ABCB5+, p63 + ABCB5+, and the differentiation control p63 + ABCB5+ CK3+ were obtained. After each sorting, aliquots for total RNA quality control were withdrawn, and the cell remainders were kept at −80°C as frozen pellets until RNA extraction, at which point subpopulations from the three different sorting runs were pooled.

Total RNA Extraction and Next-Generation Sequencing

The RNA extraction and next-generation sequencing was carried out on a commercial basis by the AROS Applied Biotechnology (Aarhus, Denmark). The technologies used were based on the QIAsymphony RNA Kit (QIAGEN, Copenhagen, Denmark) for RNA isolation and the SMART-Seq v4 Ultra Low Input RNA Kit and Low Input Library Prep Kit V2 (both from Takara Bio, Otsu, Japan) for cDNA and sequence library preparation, respectively. The RNA-seq was done using an Illumina HiSeq 2000 instrument (Illumina Inc., San Diego, CA). Quality of obtained raw sequencing data was assessed with the aid of Qualimap v2.2 [40]. The sequences were submitted to Gene Expression Omnibus (GEO, http://www. ncbi. nlm. nih. gov/geo/) under accession number PRJNA387095.

Transcript Assembly and Differential Expression Analysis

After trimming, the sequenced transcripts were imported as paired-ends reads into Cufflinks v2.21 for transcriptome assembly and differential expression analysis [41, 42]. Assembly of transcripts was performed against an annotated Homo Sapiens reference genome (Human genome 19). Six distinct RNA-seq experiments were created for each pair combination from the four hLESC phenotypic variants. These included, ABCB5+ versus p63+, p63 + ABCB5+ versus p63+, p63 + ABCB5 + CK3+ versus p63+, p63 + ABCB5+ versus ABCB5+, p63 + ABCB5+ CK3+ versus ABCB5+, and p63 + ABCB5+ CK3+ versus p63 + ABCB5+. Significance of differential gene expression was assessed at Benjamini & Hochberg false discovery rate (FDR)-adjusted *p*-values (*q*-values) <.05 [43]. InteractiVenn was used to render 4-way interactions among the independent libraries according to selected criteria [44]. CummeRbund v2.0.0 was invoked to produce heat maps of hierarchical clustering of genes and samples based on fragments per kilobase of transcript per million mapped reads (FPKM) values [45].

Gene Ontology Analysis

Significant differentially expressed genes were annotated for over-represented gene ontology (GO) terms in biological process using Database for annotation, visualization and integrated discovery (DAVID) [46, 47]. To graphically render the relationships between significantly enriched ($q < .05$) GO terms, hypergeometric tests were performed and the resulting GO categories were visualized in a network fashion using BiNGO [48] in the Cytoscape environment [49].

Statistics

Data represent the mean (± standard deviation, SD) of three independent FACS procedures. For the data that is shown in differential gene expression as well as gene ontology analyses, an FDR adjusted *p*-value (*q*-value) was applied for multiple hypothesis testing based on Benjamini-Hochberg procedure [43].

Results

Immunophenotype Analysis and RNA Isolation and Sequencing

The staining patterns of the selected antibodies were first confirmed by in situ immunofluorescence microscopy. The ABCB5 antibody produced a cell surface signal, whereas the p63 and CK3 antibodies reacted with intranuclear and cytoplasmic epitopes, respectively (Fig. 1A). The sorting was carried out from three independent cultures of hLESCs, and after averaging values from the sorted populations, the frequency of individual markers was, 31.5% ± 1.5% for p63, 27.7% ± 5.1% for ABCB5, and 43% ± 2.5% for CK3 (mean ± SD). The flow cytometric traces, which were obtained in one of the sorting experiments are shown in Figure 1B as representative data. The analysis of co-expression patterns further revealed that most of the cells did not bear any of the studied markers (40.4% ± 4.4%), and of the sorted subpopulations, the most prevalent phenotype was p63 + ABCB5 + CK3+ (red; 15.1% ± 2.9%), followed by ABCB5+ (green; 7.8% ± 3.0%), p63+ (blue; 2.9% ± 1.3%), and p63 + ABCB5+ (orange; 2.6% ± 1.3%) (Fig. 1B).

Before sequencing, the RNA quality was analyzed using parameters described previously [39], and the values pertinent to individual populations are shown in Supporting Information Table S2. Although the RNA yield varied broadly, up to 2.8-fold between the highest and lowest values, the RIN appeared consistent and sufficiently high (7.7 ± 0.4, $n = 4$) to meet the requirements of the protocol.

The analysis of the sequencing process by invoking the PHRED quality score confirmed high reliability of the obtained data, since more than 80% of all base calls scored higher than 30 (Fig. 1C). Importantly, a satisfactory depth of sequencing was achieved to perform differential expression profiling, as on average 1.14E + 08 reads were acquired per sample. More than 80% of these reads mapped in pairs, which translates into a total average of 94.27 $\times 10^6$ pair-end reads (Table 1). Additional quality parameters were explored, and they are included in Figure 1B and Table 1. In particular, the average GC content for the mapped reads was 49.25% and the GC content per sample displayed a normal distribution. All four sequence libraries exhibited expected, nearly identical log-normal profile of coverage per mapped position (FPKM), and, similarly, appeared to cover the whole genome, where on average 86.96% of the pair-end reads mapped to exonic regions of the reference human genome 19.

Differential Gene Expression Between the Sorted Cultured hLESC Subpopulations

Transcripts from the sorted subpopulations were analyzed for differential expression. Global comparison revealed that the transcriptomes were overall quite similar in terms of genes identified,

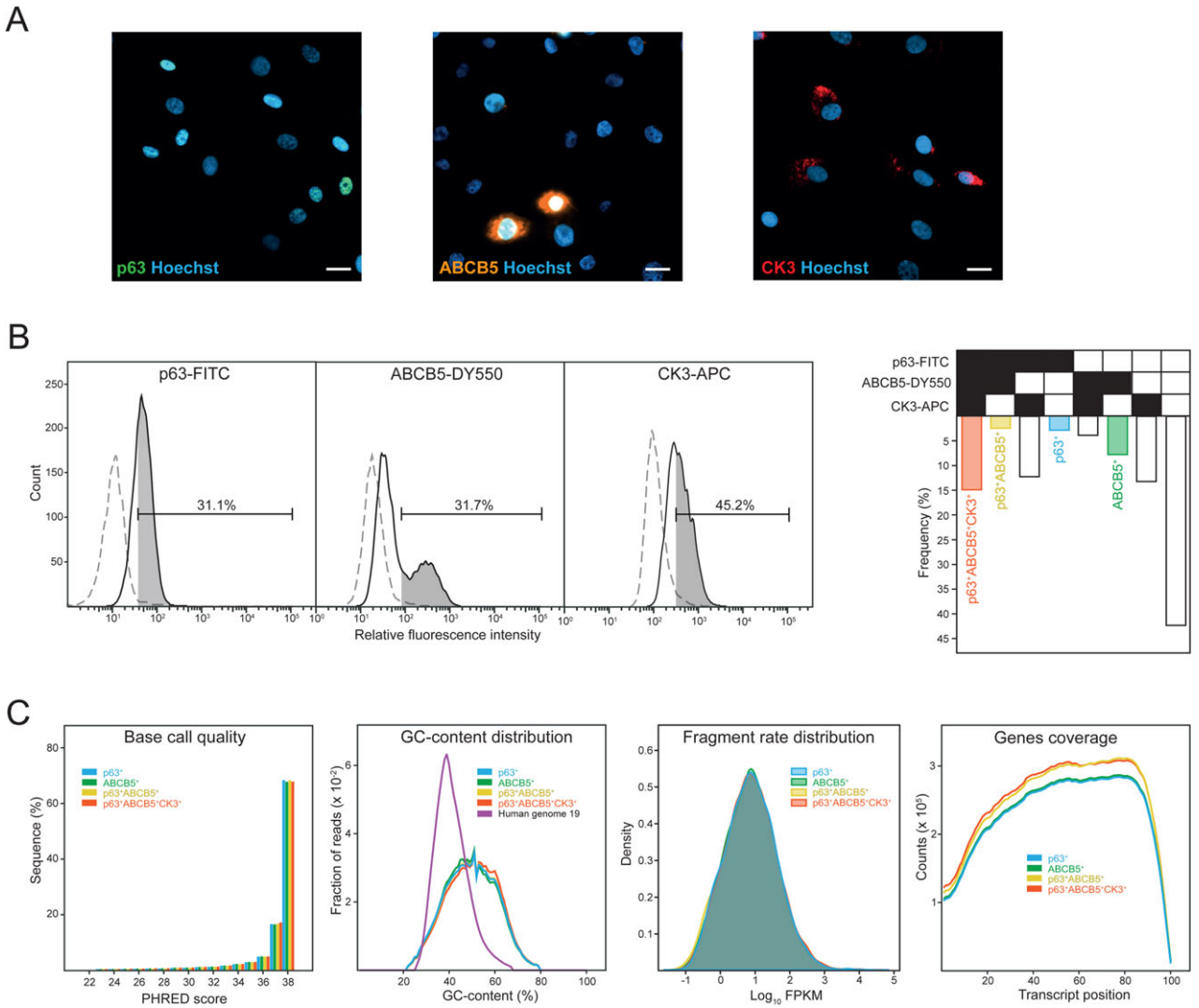

Figure 1. Identification of subpopulations and analysis of RNA sequencing. **(A):** Localization of the targeted epitopes by in situ direct immunofluorescence. The conjugates were applied to either unfixed or fixed and permeabilized cells to reveal surface (ABCB5) or intranuclear (p63) and cytoplasmic reactivity (CK3), respectively. The scale bars indicate 20 μm. **(B):** Flow cytometric data from the sorted cultured human limbal epithelial stem cells (hLESCs) population based on the three markers p63, ABCB5, and CK3. Marker positivity (grey) was based on top 2.5 percentile of control intensity (dotted line). The plots demonstrate representative data from one sorting experiment. Based on the co-expression pattern of these three markers, four subpopulations of interest, p63+ABCB5+ CK3+ (red), p63+ABCB5+ (yellow), p63+ (blue), and ABCB5+ (green), were identified and sorted. The co-expression profiles are shown as averages from three sorting experiments. **(C):** The quality of the sequencing was assessed by base call quality (PHRED score), GC-content distribution compared with the human genome 19, fragment rate distribution (log-normal profile of coverage per mapped position by fragments per kilobase million) and mapping coverage. Abbreviations: ABCB5, ATP binding cassette subfamily B member 5; CK3, cytokeratin 3; p63, protein p63.

quality of sequences and gene coverage. However, pairwise comparisons showed significant differential gene expression between the individual subpopulations (Fig. 2A,B). The actual number of significantly expressed genes ($q < .05$) regulated in either direction varied from 24 to 81, and both the up- and downregulation appeared to be in balance (Fig. 2C). The largest amount of differential regulation was observed when comparing p63 + ABCB5 +CK3+ vs. p63+ (159 genes), and the least when

Table 1. Parameters of RNA sequencing from fluorescence-activated cell sorting purified cultured human limbal epithelial stem cells subpopulations

	Reads count	Reads mapped in pairs (%)	Mapped reads GC content (%)	Reads mapped to exonic regions (%)[a]
p63+	1.23E+08	82.67	49.12	88.13
ABCB5+	1.09E+08	81.18	48.91	85.61
p63+ABCB5+	1.13E+08	82.54	49.22	85.33
p63+ABCB5+CK3+	1.11E+08	85.87	49.76	88.78

[a]Fraction out of pair-end reads mapped to human genome 19.
Abbreviation: GC, guanine-cytosine.

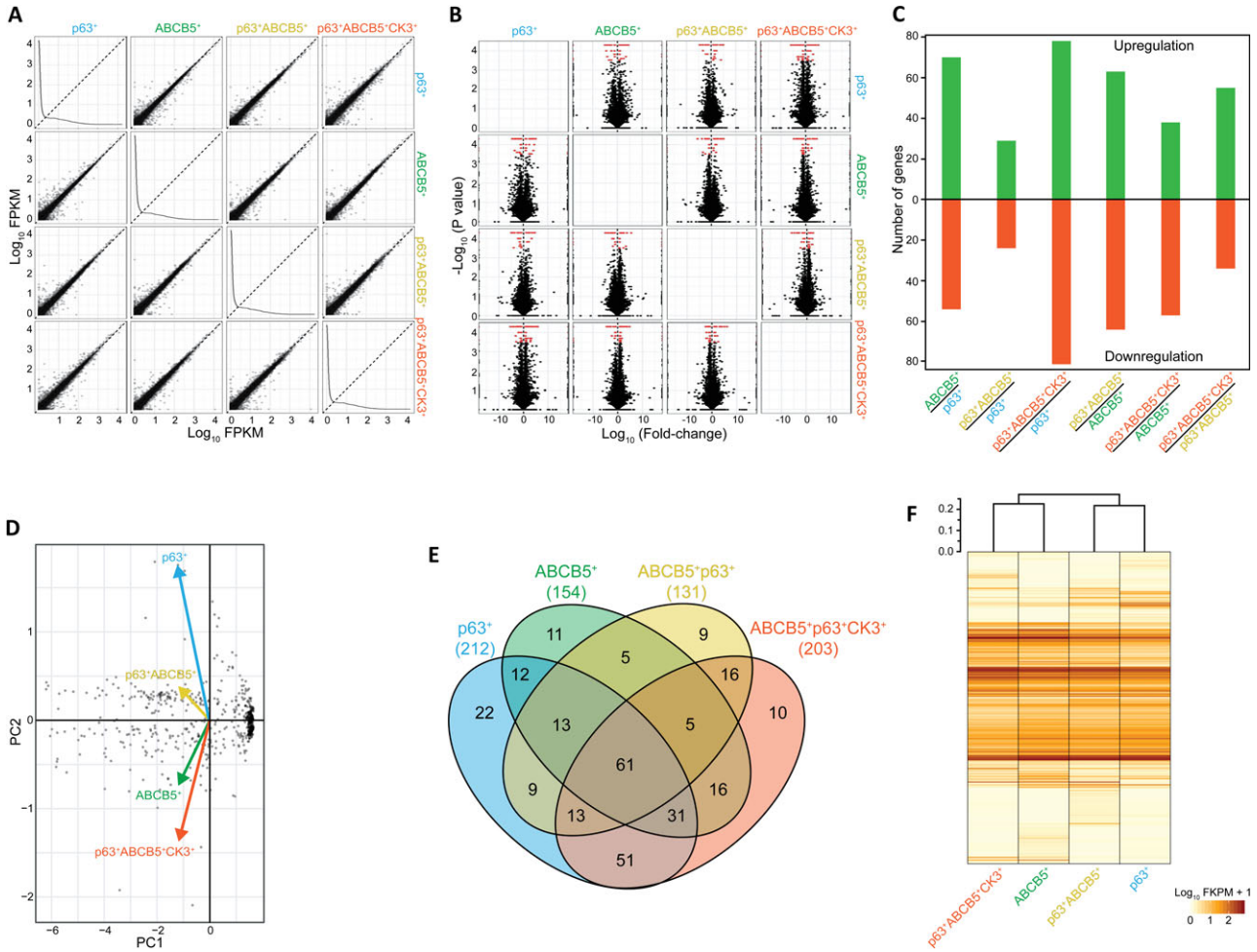

Figure 2. Differential gene expression between the sorted cultured human limbal epithelial stem cell subpopulations. **(A):** Pairwise comparison of subpopulation transcriptomes by scatter plots of all transcripts. The log2 transformed transcript abundance of all transcripts obtained are plotted against each other on the *x*-axis and *y*-axis, respectively. Each spot represents the intensity of a transcript. Diagonal line represents equal expression. **(B):** Statistical analysis of the difference between subpopulation transcripts and identification of differential regulated genes between subpopulations. The results are visualized by a scatter plot. The −log10 FDR-corrected *p*-value is plotted against the log2 fold change for each transcript. The transcripts were significantly differentially expressed between the samples ($p < .05$) are in the top (red). **(C):** Number of significantly up- (green) or downregulated (red) genes between subpopulations by pairwise comparison of subpopulations. **(D):** Principal component analysis (PCA) on the 367 most regulated genes of the transcriptomes from the four subpopulations. Shown are PCA score plots of PC1 and PC2. **(E):** Four-way Venn diagram showing the number of shared and uniquely expressed genes for the four subpopulations. **(F):** Dendrogram based on a K-means-20 cluster analysis and hierarchical alignment of differentially expressed transcripts between subpopulation based on fragments per kilobase of transcript per million mapped reads (FPKM) revealing degree of relatedness between subpopulations. Color corresponds to differential gene expression level. Genes and samples were hierarchically clustered based on Jensen-Shannon distance. Abbreviations: ABCB5, ATP binding cassette subfamily B member 5; CK3, cytokeratin 3; FPKM, fragments per kilobase million; PC1, principle component 1; PC2, principle component 2; p63, protein p63.

comparing p63 + ABCB5+ versus p63 (53 genes) subpopulations. These differences appeared sufficient to provide for a clear discrimination of the four subpopulations by principal component analysis (Fig. 2D). The co-expression patterns were further analyzed in by four-way Venn diagram plots to visualize the amount of shared and uniquely expressed genes of significance ($q < .05$) (Fig. 2E). The largest group is represented by genes that are shared by all four subpopulations (21.5%). Genes that are shared by two or three subpopulations in various combinations represent 38.4% and 21.8%, respectively, and the uniquely expressed genes represent 18.3% (Supporting Information Table S3). Since all the analyses above demonstrated that the isolated subpopulations displayed unique although closely related transcriptional activation, the degree of relatedness was explored by K-means-20 cluster analysis and hierarchical alignment (Fig. 2F). The dendrogram revealed a surprising pattern, where the ABCB5+ transcriptional signature was closer to the CK3 subpopulation than to the p63+ or p63 + ABCB5+ subpopulations. Significant differentially expressed genes ($q < .05$) were subsequently annotated for functional biological processes in the GO hierarchy.

GO Analysis

To evaluate the differentially expressed genes in terms of biological significance for a given subpopulation, functional annotations were applied using the DAVID tool. Significantly overrepresented ($q < .05$) GO terms are listed for each

Table 2. Enrichment of functional annotation terms using DAVID[a] for genes differentially expressed between the cultured human limbal epithelial stem cells subpopulations, with values <.05 after Benjamini multiple testing correction

BP_direct GO terms[b]	Fold enrichment	*p* value	Benjamini
p63+			
GO:0051301~cell division	8.27	2.78E-12	1.43E-09
GO:0008283~cell proliferation	5.14	7.89E-06	1.01E-03
GO:0008284~positive regulation of cell proliferation	4.04	8.41E-05	6.17E-03
GO:0031536~positive regulation of exit from mitosis	72.38	6.85E-04	3.02E-02
GO:0007067~mitotic nuclear division	10.51	1.05E-12	1.08E-09
GO:0051439~regulation of ubiquitin-protein ligase activity involved in mitotic cell cycle	31.47	1.67E-05	1.72E-03
GO:0051436~negative regulation of ubiquitin-protein ligase activity involved in mitotic cell cycle	10.19	1.42E-03	4.94E-02
GO:0051437~positive regulation of ubiquitin-protein ligase activity involved in regulation of mitotic cell cycle transition	11.43	1.73E-04	9.86E-03
GO:0000086~G2/M transition of mitotic cell cycle	8.45	4.34E-05	3.72E-03
GO:0000070~mitotic sister chromatid segregation	28.95	2.36E-05	2.21E-03
GO:0007062~sister chromatid cohesion	14.05	3.54E-08	9.11E-06
GO:0051983~regulation of chromosome segregation	54.28	1.27E-03	4.56E-02
GO:0007059~chromosome segregation	10.64	1.21E-03	4.52E-02
GO:0007094~mitotic spindle assembly checkpoint	28.95	3.28E-04	1.67E-02
GO:0007052~mitotic spindle organization	19.30	1.11E-03	4.30E-02
GO:0007051~spindle organization	45.24	3.57E-06	5.24E-04
GO:0051310~metaphase plate congression	48.25	6.58E-05	5.20E-03
GO:0007080~mitotic metaphase plate congression	19.56	1.16E-04	7.43E-03
GO:0031145~anaphase-promoting complex-dependent catabolic process	14.66	1.13E-06	1.95E-04
GO:0000910~cytokinesis	15.08	3.22E-04	1.73E-02
GO:0000281~mitotic cytokinesis	19.97	1.00E-03	4.05E-02
GO:0042438~melanin biosynthetic process	77.95	1.49E-10	5.12E-08
GO:0030318~melanocyte differentiation	36.19	9.29E-06	1.06E-03
GO:0048066~developmental pigmentation	62.04	9.55E-04	4.02E-02
GO:0042787~protein ubiquitination involved in ubiquitin-dependent protein catabolic process	7.57	8.75E-05	5.99E-03
GO:1901215~negative regulation of neuron death	18.09	1.58E-04	9.51E-03
GO:0007517~muscle organ development	9.76	3.62E-04	1.76E-02
GO:0030574~collagen catabolic process	18.09	2.65E-07	5.45E-05
GO:0030198~extracellular matrix organization	5.91	4.01E-04	1.86E-02
ABCB5+			
GO:0030216~keratinocyte differentiation	18.94	2.19E-08	1.47E-05
GO:0031424~keratinization	23.32	4.85E-07	8.12E-05
GO:0008544~epidermis development	16.93	5.35E-08	1.19E-05
GO:0018149~peptide crosslinking	25.59	2.29E-08	7.66E-06
p63+ABCB5+			
GO:0030199~collagen fibril organization	31.31	2.65E-04	2.27E-02
GO:0030574~collagen catabolic process	42.93	2.57E-11	1.33E-08
GO:0070208~protein heterotrimerization	87.23	1.12E-05	1.93E-03
GO:0030198~extracellular matrix organization	12.46	2.95E-06	7.67E-04
GO:0071230~cellular response to amino acid stimulus	32.48	1.54E-05	2.00E-03
GO:0007155~cell adhesion	5.99	1.01E-04	1.05E-02
GO:0001649~osteoblast differentiation	14.68	3.46E-04	2.54E-02
p63+ABCB5+CK3+			
GO:0030216~keratinocyte differentiation	18.04	2.72E-07	2.04E-04
GO:0031424~keratinization	17.85	1.68E-04	2.48E-02
GO:0008544~epidermis development	12.10	1.32E-04	2.44E-02
GO:0018149~peptide crosslinking	20.56	1.00E-05	3.74E-03
GO:0010951~negative regulation of endopeptidase activity	9.91	7.16E-05	1.77E-02

[a]Database for annotation, visualization, and integrated discovery.
Subset of biological process gene ontology terms.
Abbreviations: ABCB5, ATP binding cassette subfamily B member 5; CK3, cytokeratin 3; p63, protein p63.

subpopulation in Table 2. The GO terms pertinent to stem or progenitor cells, such as "positive regulation of exit from mitosis," "regulation of chromosome segregation," or "spindle organization" were markedly enriched in the p63+ subpopulation. Another noticeable finding in this group was that the pigmentation-related processes, such as "melanin biosynthetic process" or "developmental pigmentation," scored among the highest overrepresented terms. As expected, the terms relevant to cell differentiation, such as keratinocyte differentiation or keratinization were enriched in p63 + ABCB5+ CK3+ subpopulation. Surprisingly, however, they were found enriched practically to the same degree also in ABCB5+ subpopulation. As for the double marker-expressing p63 + ABCB5+ subpopulation, the most notable processes were those that were found in the single marker p63+ and the ABCB5+ associated with extracellular matrix and collagen metabolism.

Further understanding of the implications of above described biological processes for the relationship between the subpopulations was provided by constructing GO networks with the aid of BiNGO tool (Fig. 3). A pairwise comparison clearly demonstrates that the p63+ subpopulation is set apart by a predominance of pigmentation-associated processes,

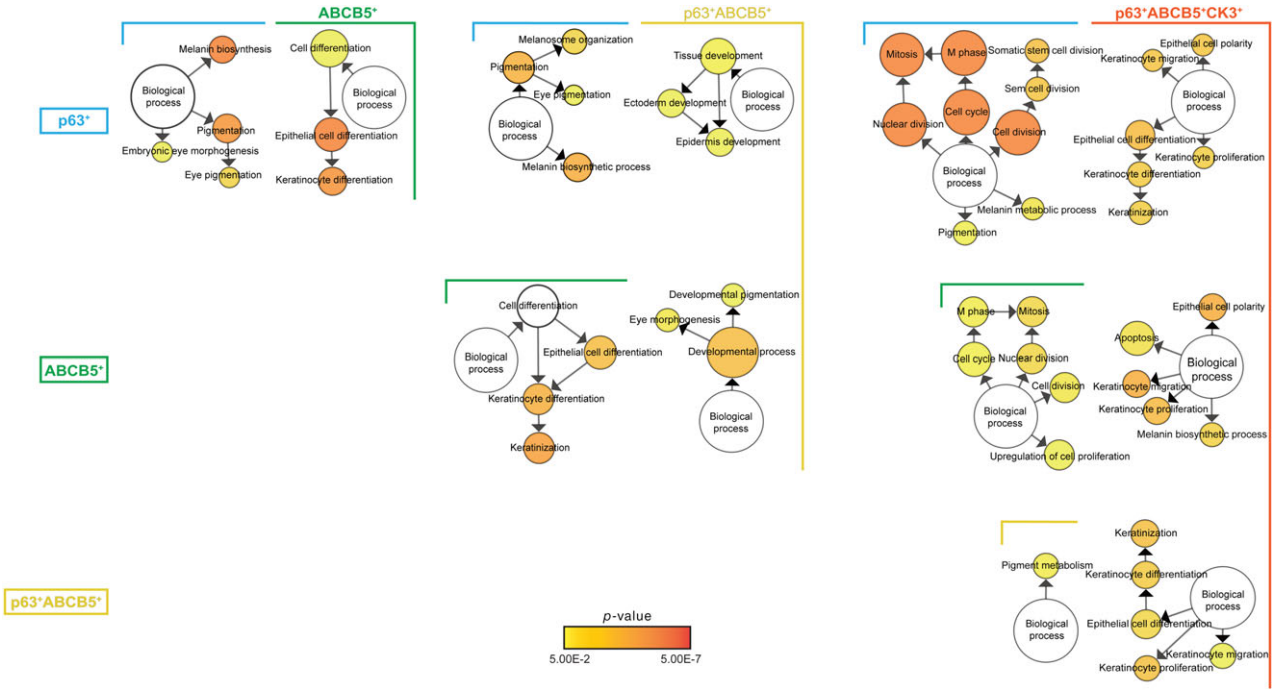

Figure 3. Biological processes of stemness and pigmentation. Gene ontology (GO) analysis of the biological processes of the upregulated genes related to stem cell and pigmentation based on pairwise comparison of the four subpopulations. The analysis was performed in Cytoscape using the BiNGO plug-in version 3.0.3. Presented is a reduced network showing the upregulated biological process categories that were significantly over-represented based on the genes identified. The color scale indicates the level of significance of the overrepresented GO category (adjusted $p < .05$). The size of the circles is proportional to the number of genes in each category. Abbreviations: ABCB5, ATP binding cassette subfamily B member 5; CK3, cytokeratin 3; p63, protein p63.

whereas all the other subpopulations are subject to epithelial-specific differentiation. This indicates that the p63+ variant is the common progenitor phenotype. On the other hand, as expected due to the expression of cytokeratin, the p63 + ABCB5+ CK3+ variant represents the most differentiated phenotype. Looking at the remaining two variants, the ABCB5+ and p63 + ABCB5+, intriguingly we found that the former phenotype appears developmentally downstream from the latter one. These relationships thus provided for a framework, upon which we based our proposal for a developmental hierarchy within the limbal niche (Fig. 4). We hypothesize that within the scope of studied phenotype variants, the p63+ represents the most immature progenitor, and the ABCB5+ marker either alone or in co-expression pattern identifies progressively more committed precursors.

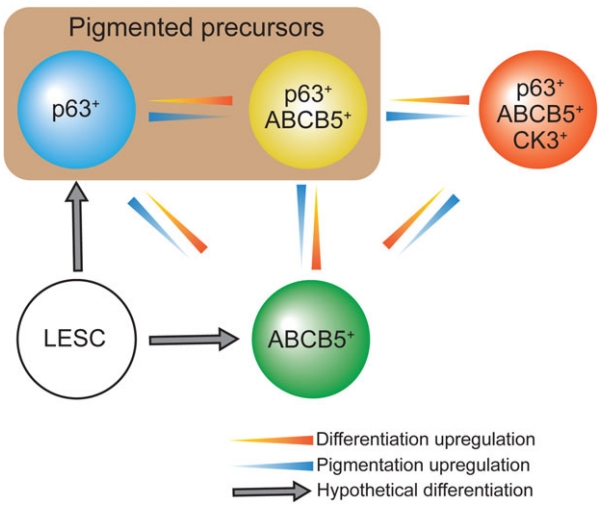

Figure 4. Association between pigmentation and stemness. Developmental hierarchy within the cultured limbal epithelial cells based on correlation of pigmentation and cell differentiation observed among hLESCs phenotypic subpopulations. Orange arrows indicate more differentiated cells; blue arrows indicate more pigmented cells. The p63+ represents the most immature progenitor, and the ABCB5 marker either alone or in co-expression pattern identifies progressively more committed precursors. Abbreviations: ABCB5, ATP binding cassette subfamily B member 5; CK3, cytokeratin 3; LESC, limbal epithelial stem cells; p63, protein p63.

Discussion

The gene ontology analysis revealed that pigmentation and epithelial differentiation were mutually exclusive processes, which enabled us to determine a developmental hierarchy within the sample of isolated cultured hLESC phenotypical variants. Intriguingly, the most immature phenotype was found associated with p63 as a single marker, whereas ABCB5 alone or in co-expression was found on the descendant variants. Relationship between melanin pigmentation and limbal stemness has previously been investigated, and interestingly, the initial indication of the presence of hLESCs was inspired by observation of pigment movement from the limbus toward epithelial defect in wounded corneas [50]. In situ, the limbal palisades of Vogt, which contain pigment granules that are aligned with the microplicae of the corneal epithelium, are believed to be the source of hLESCs [51].

The physiological significance of the elaborate melanin production and distribution in the stem cell niche has been

attributed to the protection from ultraviolet radiation and oxidative damage [52, 53]. Melanocytes that can be found scattered in the basal limbus epithelium have been highlighted as a major site of pigment production [54–57], nevertheless, our current investigation, in line with some previous studies, demonstrates that the limbal corneal progenitors are by themselves involved in melanin turnover [19, 32, 58]. Importantly, a direct communication between both cell lineages has as well as been documented [52–54]. This observation thus provides structural basis for realization that a cellular network, possibly also including players from additional compartments, that entails a comprehensive crosstalk is essential in order to properly maintain the limbal niche.

Although the molecular basis for the relationship between pigmentation and the hLESC maintenance or p63 is not fully understood, there is a plethora of evidence that implicates the *SERPINF1*, which encodes the pigment epithelium-derived factor (PEDF). PEDF was first identified as a 50 kDa secreted protein in conditioned medium from cultured fetal human retinal pigment epithelium (RPE) cells [59], and was recognized as a potent inhibitor of vascular endothelial growth factor (VEGF) [60]. Recently, PEDF was proposed to regulate the proliferation and differentiation of human embryonic stem cells[61] as well as multiple tissue-specific stem cells [62], and was also found in developing and mature human cornea [58]. With regard to hLESCs, it has been reported that the PEDF has the capacity to promote self-renewal [17] and that such effect may be associated with the p63 expression [63]. PEDF's effect on regeneration of a functional limbus was further confirmed by Yeh et al. in 2016 in the rabbit model of LSCD [64, 65]. Interestingly, a possible regulatory mechanism was unveiled, when the PEDF was reported to be a direct target gene for p63 [66]. The results from our current investigation provide additional support for the PEDF role by demonstrating its exclusive association with earliest developmental phenotype, which is marked by single p63 expression.

Based on our model of differentiation hierarchy within the cultured limbal epithelial cells, the ABCB5 designates a lineage that is still of a precursor type, but is clearly distinct from the pigmented lineage that is associated with p63. Previously, based on the morphological criteria, differentially pigmented precursor types have been identified in the palisades of Vogt and in the transition zone closer to the peripheral cornea [67, 68]. It is highly likely, that the phenotypical variants analyzed in our study correspond to the in situ progenitors from the above studies, nevertheless, only direct identification of the place of residence within the limbus of the four studied phenotypes can give a definitive answer. Such study would undoubtedly shed more light on the developmental relationship between p63 and ABCB5 as well as the role of pigmentation in the maintenance of the limbal niche.

Conclusion

Both p63 and ABCB5 have been well established as markers associated with limbal stemness, nevertheless, their placement within the differentiation hierarchy has not been known until now. Although we were not able to confirm that the variant bearing single p63 corresponds to the true limbal stem cell, we have demonstrated that it is a more immature progenitor than those featuring ABCB5 alone or in co-expression patterns. Building on our approach, and invoking phenotypes with complex marker repertoires, it may be possible to infer in high detail the developmental hierarchy relevant for the limbal niche. Such knowledge will in turn have practical implications, so that the perspective treatments would be based on the rational selection of the earliest progenitors available.

Acknowledgments

L.L. is supported by China Scholarship Council and S.C. Van Fonden. The flow cytometer was purchased by a donation from the Obelske Family foundation.

Author Contributions

L.L.: conception and design, collection and assembly of data, data analysis and interpretation, manuscript writing, final approval of manuscript; F.M.N.: collection of data, final approval of manuscript; J.E., S.R., T.F., and C.P.P.: data analysis and interpretation, manuscript writing, final approval of manuscript; C.B.: conception and design, final approval of manuscript; J.Ø.H.: provision of study materials, final approval of manuscript; V.Z.: conception and design, financial support, data analysis and interpretation, manuscript writing, final approval of manuscript.

Disclosure of Potential Conflicts of Interest

The authors indicated no potential conflicts of interest.

References

1 Tseng SC. Concept and application of limbal stem cells. Eye (Lond) 1989;3:141–157.
2 Haagdorens M, Van Acker SI, Van Gerwen V et al. Limbal stem cell deficiency: Current treatment options and emerging therapies. Stem Cells Int 2016; 2016:1–22.
3 Pellegrini G, Traverso CE, Franzi A. T et al. Long-term restoration of damaged corneal surfaces with autologous cultivated corneal epithelium. Lancet 1997;349:990–993.
4 Ramachandran C, Basu S, Sangwan VS et al. Concise review: The coming of age of stem cell treatment for corneal surface damage. Stem Cells Translational Medicine 2014; 3:1160–1168.
5 Rama P, Matuska S, Paganoni G et al. Limbal stem-cell therapy and long-term corneal regeneration. N Engl J Med 2010;363: 147–155.
6 Baylis O, Figueiredo F, Henein C et al. 13 years of cultured limbal epithelial cell therapy: A review of the outcomes. J Cell Biochem 2011;112:993–1002.
7 Di Iorio E,Ferrari S, Fasolo A et al. Techniques for culture and assessment of limbal stem cell grafts. Ocul Surf 2010;8:146–153.
8 Nakamura T, Inatomi T, Sotozono C et al. Ocular surface reconstruction using stem cell and tissue engineering. Prog Retin Eye Res 2016;51:187–207.
9 Pellegrini G, Dellambra E, Golisano O et al. P63 identifies keratinocyte stem cells. Proc Natl Acad Sci USA 2001;98:3156–3161.
10 Dolgin E. Next-generation stem cell therapy poised to enter EU market. Nat Biotechnol 2015;33:224–225.

11 Pellegrini G, Lambiase A, Macaluso C et al. From discovery to approval of an advanced therapy medicinal product-containing stem cells, in the EU. Regen Med 2016;11:407–420.
12 Ksander BR, Kolovou PE, Wilson BJ et al. ABCB5 is a limbal stem cell gene required for corneal development and repair. Nature 2014;511:353–357.
13 Wang Z, Zhou Q, Duan H et al. Immunological properties of corneal epithelial-like cells derived from human embryonic stem cells. PLoS One 2016;11:e0150731.
14 Shaharuddin B, Ahmad S, Md Latar N et al. A human corneal epithelial cell line model for limbal stem cell biology and limbal immunobiology. Stem Cells Translational Medicine 2017;6:761. sctm.2016-0175.
15 Barbaro V, Testa A, Di Iorio E et al. C/EBPdelta regulates cell cycle and self-renewal of human limbal stem cells. J Cell Biol 2007;177:1037–1049.
16 Serna-Ojeda JC, Graue-Hernandez EO, Navas A et al. Expanded allogeneic limbal stem cell transplantation for diverse severe limbal stem cell deficiency, investigation of ABCB5 and deltaNp63-alpha markers. Invest Ophthalmol Vis Sci 2016;57:902–902.
17 Kulkarni BB, Tighe PJ, Mohammed I et al. Comparative transcriptional profiling of the limbal epithelial crypt demonstrates its putative stem cell niche characteristics. BMC Genomics 2010;11:526.
18 Nakatsu MN, Vartanyan L, Vu DM et al. Preferential biological processes in the human limbus by differential gene profiling. PLoS One 2013;8:e61833.
19 Takács L, Tóth E, Losonczy G et al. Differentially expressed genes associated with human limbal epithelial phenotypes: New molecules that potentially facilitate selection of stem cell-enriched populations. Invest Opthalmology Vis Sci 2011;52:1252.
20 Greco D, Vellonen K-S, Turner HC et al. Gene expression analysis in SV-40 immortalized human corneal epithelial cells cultured with an air-liquid interface. Mol Vis 2010;16:2109–2120.
21 Nieto-Miguel T, Calonge M, de la Mata A et al. A comparison of stem cell-related gene expression in the progenitor-rich limbal epithelium and the differentiating central corneal epithelium. Mol Vis 2011;17:2102–2117.
22 Paaske Utheim T,Salvanos P, Aass Utheim Ø et al. Transcriptome analysis of cultured limbal epithelial cells on an intact amniotic membrane following hypothermic storage in optisol-GS. J Funct Biomater 2016; 7:4.
23 Mutz K-O, Heilkenbrinker A, Lönne M et al. Transcriptome analysis using next-generation sequencing. Curr Opin Biotechnol 2013;24:22–30.
24 Schlötzer-Schrehardt U, Kruse FE. Identification and characterization of limbal stem cells. Exp Eye Res 2005;81:247–264.
25 Kasetti RB, Gaddipati S, Tian S et al. Study of corneal epithelial progenitor origin and the Yap1 requirement using keratin 12 lineage tracing transgenic mice. Sci Rep 2016;6: 35202.
26 Li J, Xiao Y, Coursey TG et al. Identification for differential localization of putative corneal epithelial stem cells in mouse and human. Sci Rep 2017;7:5169.
27 Sun T-T, Lavker RM. Corneal epithelial stem cells: Past, present, and future. J Invest Dermatol Symp Proc 2004;9:202–207.
28 Lehrer MS, Sun TT, Lavker RM. Strategies of epithelial repair: Modulation of stem cell and transit amplifying cell proliferation. J Cell Sci 1998;111:2867–2875.
29 Barbaro V, Testa A, Di Iorio E et al. C/EBPdelta regulates cell cycle and self-renewal of human limbal stem cells. J Cell Biol 2007;177:1037–1049.
30 Romano AC, Espana EM, Yoo SH et al. Different cell sizes in human limbal and central corneal basal epithelia measured by confocal microscopy and flow cytometry. Invest Ophthalmol Vis Sci 2003;44: 5125–5129.
31 Nakamura T, Kelly JG, Trevisan J et al. Microspectroscopy of spectral biomarkers associated with human corneal stem cells. Mol Vis 2010;16:359–368.
32 Bath C, Muttuvelu D, Emmersen J et al. Transcriptional dissection of human limbal niche compartments by massive parallel sequencing. PLoS One 2013;8:e64244.
33 Carnes MU, Allingham RR, Ashley-Koch A et al. Transcriptome analysis of adult and fetal trabecular meshwork, cornea, and ciliary body tissues by RNA sequencing. Exp Eye Res 2018;167:91–99
34 Bath C, Fink T, Vorum H et al. Technical brief: Optimized pipeline for isolation of high-quality RNA from corneal cell subpopulations. Mol Vis 2014;20:797–803.
35 Kameishi S, Umemoto T, Matsuzaki Y et al. Characterization of rabbit limbal epithelial side population cells using RNA sequencing and single-cell qRT-PCR. 2016;473: 704–709.
36 Sartaj R, Zhang C, Wan P et al. Characterization of slow cycling corneal limbal epithelial cells identifies putative stem cell markers. Sci Rep 2017;7:3793.
37 Liu L, Nielsen FM, Riis SE et al. Maintaining RNA integrity for transcriptomic profiling of ex vivo cultured limbal epithelial stem cells after fluorescence-activated cell sorting (FACS). Biol Proced Online 2017;19:15.
38 Bath C, Yang S, Muttuvelu D et al. Hypoxia is a key regulator of limbal epithelial stem cell growth and differentiation. Stem Cell Res 2013;10:349–360.
39 Liu L, Nielsen FM, Riis SE et al. Maintaining RNA integrity for transcriptomic profiling of ex vivo cultured limbal epithelial stem cells after fluorescence-activated cell sorting (FACS). Biol Proced Online 2017; 19:15.
40 Okonechnikov K, Conesa A, García-Alcalde F. Qualimap 2: Advanced multi-sample quality control for high-throughput sequencing data. Bioinformatics 2015;32: 292–294.
41 Trapnell C, Williams BA, Pertea G et al. Transcript assembly and quantification by RNA-Seq reveals unannotated transcripts and isoform switching during cell differentiation. Nat Biotechnol 2010;28:511–515.
42 Trapnell C, Hendrickson DG, Sauvageau M et al. Differential analysis of gene regulation at transcript resolution with RNA-seq. Nat Biotechnol 2013;31:46–53.
43 Benjamini Y, Hochberg Y. Controlling the false discovery rate: A practical and powerful approach to multiple testing. J R Stat Soc Ser B 1995;57:289–300.
44 Heberle H, Meirelles GV, da Silva FR et al. InteractiVenn: A web-based tool for the analysis of sets through Venn diagrams. BMC Bioinform 2015;16:169.
45 Goff LA, Trapnell C, Kelley D. cummeRbund: Analysis, exploration, manipulation, and visualization of Cufflinks high-throughput sequencing data. http://compbio.mit.edu/cummeRbund/ (2012).
46 Huang DW, Sherman BT, Lempicki RA. Systematic and integrative analysis of large gene lists using DAVID bioinformatics resources. Nat Protoc 2009;4:44–57.
47 Huang DW, Sherman BT, Lempicki RA. Bioinformatics enrichment tools: paths toward the comprehensive functional analysis of large gene lists. Nucleic Acids Res 2009; 37:1–13.
48 Maere S, Heymans K, Kuiper M. BiNGO: A Cytoscape plugin to assess overrepresentation of gene ontology categories in Biological Networks. Bioinformatics 2005;21:3448–3449.
49 Shannon P, Markiel A, Ozier O et al. Cytoscape: A software environment for integrated models of biomolecular interaction networks. Genome Res 2003;13:2498–2504.
50 Mann I. A study of epithelial regeneration in the living eye. Br J Ophthalmol 1944; 28:26–40.
51 Schermer A, Galvin S, Sun TT. Differentiation-related expression of a major 64K corneal keratin in vivo and in culture suggests limbal location of corneal epithelial stem cells. J Cell Biol 1986;103:49–62.
52 Higa K, Shimmura S, Miyashita H et al. Melanocytes in the corneal limbus interact with K19-positive basal epithelial cells. Exp Eye Res 2005;81:218–223.
53 Hayashi R, Yamato M, Sugiyama H et al. N-cadherin is expressed by putative stem/progenitor cells and melanocytes in the human limbal epithelial stem cell niche. Stem Cells 2007;25:289–296.
54 Secker GA, Daniels JT, Sight C. Limbal epithelial stem cells of the cornea. StemBook 2009;1–18.
55 Li Y, Inoue T, Takamatsu F et al. Differences between niche cells and limbal stromal cells in maintenance of corneal limbal stem cells. Invest Opthalmol Vis Sci 2014;55:1453.
56 Dziasko MA, Armer HE, Levis HJ et al. Localisation of epithelial cells capable of holoclone formation in vitro and direct interaction with stromal cells in the native human limbal crypt. PLoS One 2014;9:e94283.
57 Dziasko MA, Tuft SJ, Daniels JT. Limbal melanocytes support limbal epithelial stem cells in 2D and 3D microenvironments. Exp Eye Res 2015;138:70–79.
58 Ding Z, Dong J, Liu J et al. Preferential gene expression in the limbus of the vervet monkey. Mol Vis 2008;14:2031–2041.
59 Tombran-Tink J, Chader GG, Johnson LV. PEDF: A pigment epithelium-derived factor with potent neuronal differentiative activity. Exp Eye Res 1991;53:411–414.
60 Bhutto IA, McLeod DS, Hasegawa T et al. Pigment epithelium-derived factor (PEDF) and vascular endothelial growth factor (VEGF) in aged human choroid and eyes with

age-related macular degeneration. Exp Eye Res 2006;82:99–110.
61 Gonzalez R, Jennings LL, Knuth M et al. Screening the mammalian extracellular proteome for regulators of embryonic human stem cell pluripotency. Proc Natl Acad Sci USA 2010;107:3552–3557.
62 Sagheer U, Gong J, Chung C. Pigment epithelium-derived factor (PEDF) is a determinant of stem cell fate: Lessons from an ultrarare disease. J Dev Biol 2015;3:112–128.
63 Ho T-C, Chen S-L, Wu J-Y et al. PEDF promotes self-renewal of limbal stem cell and accelerates corneal epithelial wound healing. Stem Cells 2013;31:1775–1784.
64 Yeh S-I, Ho T-C, Chen S-L et al. Pigment epithelial-derived factor peptide facilitates the regeneration of a functional limbus in rabbit partial limbal deficiency. Investig Opthalmol Vis Sci 2015;56:2126.
65 Yeh S-I, Ho T-C, Chen S-L et al. Pigment epithelial-derived factor peptide regenerated limbus serves as regeneration source for limbal regeneration in rabbit limbal deficiency. Invest Opthalmol Vis Sci 2016;57:2629.
66 Sasaki Y, Naishiro Y, Oshima Y et al. Identification of pigment epithelium-derived factor as a direct target of the p53 family member genes. Oncogene 2005;24:5131–5136.
67 Schlötzer-Schrehardt U, Kruse FE. Identification and characterization of limbal stem cells. Exp Eye Res 2005;81:247–264.
68 Lauweryns B, van den Oord JJ, De Vos R et al. A new epithelial cell type in the human cornea. Invest Ophthalmol Vis Sci 1993;34:1983–1990.


See www.StemCells.com for supporting information available online.

